

Freestanding Three-Dimensional Copper Foils Prepared by Electroless Deposition on Micropatterned Gels**

By Stoyan K. Smoukov, Kyle J. M. Bishop, Christopher J. Campbell, and Bartosz A. Grzybowski*

Microstructured metal foils are important components of several modern technologies, with applications in magnetic disk-drive heads,^[1] NMR microcoils,^[2,3] and micro/nanoelectronic devices.^[4,5] The combination of their mechanical rigidity and high thermal conductivity makes them useful components of microelectromechanical systems (MEMS),^[6,7] microfluidic pumps and valves,^[8] nanofluidic channels,^[9] and microelectrodes for electrophoretic-chip sensing.^[10] Metal sheets have also been used as masks for chemical and dry etching^[11] and as selective membranes with desirable catalytic properties.^[12,13] While the majority of these applications use planar micropatterned foils, there has recently been a growing interest in preparing three-dimensional (3D) metallic microstructures which are interesting in the context of lightweight materials,^[9,14] microwaveguides,^[15,16] and as structural and electrical components of microrobots.^[17]

Existing methods for the fabrication of micropatterned 3D metal sheets include thermal evaporation, electron-beam evaporation,^[18] sputtering,^[19] and metal-organic chemical vapor deposition (MOCVD).^[20] These techniques require expensive, high-vacuum instrumentation and are limited to “line-of-sight” deposition, thus making metallization of vertical walls or features with negative inclines difficult. Electroplating can be used to metallize diverse 3D topographies, but is limited to use on conductive surfaces from which the foils cannot be easily detached.^[21] This limitation is also present in the technologically important LIGA (“lithographie, galvanof ormung, abformung” i.e., lithography, electroforming, casting) process, which was used to prepare some intricate high-aspect-ratio microstructures.^[15,22]

Electroless deposition has been successful at generating two-dimensional (2D) micropatterned films on a variety of surfaces (e.g., Si/SiO₂, glass,^[23] polyimide,^[23,24] polystyrene^[24]), but has not been extended to 3D topographies, save smooth surfaces with macroscopic 3D features.^[25] Other techniques for generating 3D structures involve meticulous manual folding and welding of patterned 2D films.^[26,27]

Here, we describe a versatile and reliable method based on electroless plating that overcomes many of these limitations, and allows preparation of either freestanding or polymer-supported 3D copper films with complex topographies. In our method (Fig. 1), metal is deposited on the surface of a rectangular block of a hydrogel micropatterned in bas-relief. This block was first soaked in solutions of an electroless-plating sensitizer and activator, and then immersed in a copper-plating solution. Ensuing electroless deposition gave foils that were mechanically rugged and detached easily from the gel support. By directing diffusional fluxes at the surface of agarose, we were able to selectively metallize different portions

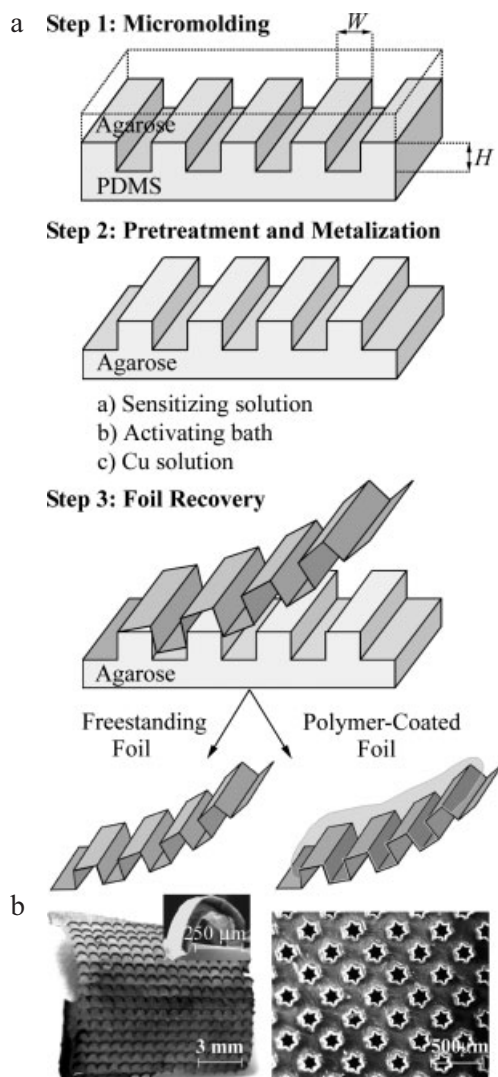


Figure 1. a) The scheme illustrates preparation of freestanding and polymer-supported 3D copper foils, and gives pertinent dimensions ($W \sim 20\text{--}250 \mu\text{m}$, $H \sim 40\text{--}400 \mu\text{m}$, $H/W \sim 0.4\text{--}2$). After plating, thicker foils were peeled off the masters to give freestanding films and thinner foils were transferred onto and supported by a photocurable resin. b) Examples of continuous (left) and membrane-like (right) foils. The inset in the left picture is a scanning electron microscope (SEM) image of a wiggly line detached from the foil and viewed from the back side.

[*] Prof. Dr. B. A. Grzybowski, Dr. S. K. Smoukov, K. J. M. Bishop, C. J. Campbell
Department of Chemical and Biological Engineering
Northwestern University
2145 Sheridan Rd, Evanston, IL 60208 (USA)
E-mail: grzybor@northwestern.edu

[**] B. A. G. gratefully acknowledges financial support from Northwestern University start-up funds and from the Camille and Henry Dreyfus New Faculty Awards Program. Supporting Information is available online from Wiley InterScience or from the author.

of the micropattern embossed on the gel surface, and thus to prepare either continuous or membrane-like films (Fig. 1b). Furthermore, by adjusting the sizes of the catalytic seeds formed in situ in the agarose stamps, we were able to control the roughness of the plated films. Our work demonstrates that reaction-diffusion phenomena can provide a basis for new types of flexible microfabrication approaches.

3D copper foils were fabricated according to the procedure outlined in Figure 1a, and detailed in the Experimental section. Briefly, a hot, degassed 4–12 % w/w solution of agarose (OmniPur Agarose, Darmstadt, Germany) in deionized water was cast against a plasma-oxidized poly(dimethylsiloxane) (PDMS) master that had an array of raised features embossed on its surface (typical feature size, $W \sim 20\text{--}250 \mu\text{m}$; feature depth, $H \sim 40\text{--}400 \mu\text{m}$; $H/W \sim 0.4\text{--}2$). After degassing under vacuum and gelation, the agarose layer was gently peeled off, and cut into $\sim 2 \text{ cm} \times 2 \text{ cm} \times 2 \text{ mm}$ rectangular blocks (gel masters) patterned with the negative of the array of the features in the PDMS master. Next, the gel masters were soaked in an aqueous sensitizing solution (5 g L^{-1} SnCl_2 , 40 mL L^{-1} HCl 37 % assay, pH 0.8) for $t_{\text{sens}} = 2\text{--}48 \text{ h}$, washed in deionized water for $t_{\text{wash}} = 10 \text{ min--}24 \text{ h}$, and soaked in an aqueous activating solution (2.5 mL L^{-1} of a 2 % w/v PdCl_2 solution, 1.0 mL L^{-1} HCl 37 % assay, pH 1.7) for $t_{\text{activ}} = 5 \text{ min--}2 \text{ h}$. Finally, the masters were transferred into a copper plating solution made by dissolving $\text{C}_4\text{H}_4\text{KNaO}_6 \cdot 4\text{H}_2\text{O}$ (potassium sodium tartrate) (25 g L^{-1}) and KOH (12.5 g L^{-1}), adding anhydrous CuSO_4 (5 g L^{-1}), and mixing in an aqueous solution of formaldehyde (12.5 mL L^{-1} or 25.0 mL L^{-1} of a 37 % solution).^[28]

A continuous, conductive, copper film developed on the stamp's surface within $t_{\text{plate}} = 30\text{--}60 \text{ min}$ from the beginning of plating. At $t_{\text{plate}} = 90\text{--}120 \text{ min}$, this film ($\sim 0.5\text{--}1 \mu\text{m}$ thick) could be transferred, intact, onto a polymeric support by covering the surface of the stamp with a photocurable polyurethane resin (Norland Optical Adhesive 63), crosslinking it using 366 nm radiation^[29] for 15 min, and gently peeling it off. Preparation of freestanding films (at least 2–5 μm thick) required longer plating times (typically 24–48 h, with refreshing the plating solution every 12 h). These films peeled off neatly from the high-percentage agarose stamps (8–12 %). Colloidal particles of Cu rooted near the surface in the gel matrix caused a thin ($\sim 2 \mu\text{m}$) film of agarose to transfer along with the metal foil. In lower-percentage stamps, this gel layer was thicker ($\sim 10 \mu\text{m}$) and the lower strength of the matrix caused pieces of gel to break off with the peeling foil. However, this gel layer could be removed later by washing with dilute HCl and ultrasonication.

Both the roughness (from the side of the gel support—the “back side”) and the topographies of the 3D foils could be controlled by adjusting the times of activation and plating. Qualitatively, roughness depended on t_{activ} , while t_{plate} determined which portions of the surface metallized. These effects can be explained by the diffusion of participating chemicals towards the metallizing gel surface from the gel's bulk and from the plating solution, respectively.

Film roughness: The roughness of the back sides of the foils increased with increasing times of soaking in the activating Pd solution, t_{activ} , and varied only slightly with t_{sens} and t_{wash} . This trend is illustrated in Figure 2a, which shows statistics of the heights—which were derived from atomic force microscopy (AFM)—of the surface deformations for four Cu foils prepared under different experimental conditions. The foils formed on stamps that were soaked for 15 min were substantially smoother (root-mean-square (RMS) roughness $\sim 30\text{--}40 \text{ nm}$) than those prepared on stamps soaked for 2 h (RMS roughness $\sim 70\text{--}80 \text{ nm}$).

These observations are explained by a reaction-diffusion model that relates the roughness of the foils to the sizes of the colloidal seeds that initiate plating at the gel's surface. Briefly, when the stamp is initially soaked in a sensitizing solution and subsequently washed in water, a gradient of $[\text{Sn}^{2+}]$ is established in the gel, with the concentration of Sn^{2+} increasing with distance from the gel's surface, x (Fig. 2b). Upon immersion in the activating solution, Pd^{2+} cations diffuse into the gel and react (in a diffusion-limited reaction) with Sn^{2+} in a 1:3 stoichiometry, to form colloidal complexes consisting of a metallic Sn/Pd core stabilized by strongly adhered Sn^{2+} .^[30] Before the formation of the stabilizing layer, these complexes were free to aggregate and form larger particles whose radii, R , are characterized by an exponential distribution, $F(R) = \exp(-R/R_{\text{av}})/R_{\text{av}}$, where $R_{\text{av}} \sim 1.5 \text{ nm}$ is the mean particle radius.^[31,32] The Pd/Sn particles of various sizes diffused through the gel matrix. Their diffusivities, D_{g} , are given by the Stokes–Einstein equation corrected for the gel environment:^[33]

$$D_{\text{g}} = D_{\text{o}} \left[1 + \frac{2\varphi}{3} \left(\frac{r_{\text{s}} + r_{\text{f}}}{r_{\text{f}}} \right)^2 \right]^{-1} \exp\left(-\pi\varphi^{0.174 \ln(59.6 r_{\text{f}}/r_{\text{s}})}\right) \quad (1)$$

in which $D_{\text{o}} = k_{\text{B}}T/6\pi\mu R$ is the diffusivity in solution, $\varphi = (\text{gel concentration})/1.025$ is the volume fraction of the gel,^[34] $r_{\text{f}} = 0.6 \text{ nm}$ is the fiber radius in the gel,^[33] r_{s} is the radius of the diffusing particles, k_{B} is the Boltzmann constant, μ is the fluid viscosity, and T is the temperature. Approximating the gel as a semi-infinite slab, the reaction-diffusion phenomena are described by a set of partial differential equations, given in the Supporting Information.

The time-dependent solutions of these equations for the distribution of the Pd/Sn particles in the gel are widening bell-shaped curves. Curves corresponding to smaller particles widen more rapidly than those corresponding to larger ones (Fig. 2b). In other words, for short soaking times, it is mostly the small particles that reach the gel surface. For longer times, the small particles diffuse out of the gel, and it is mostly the larger ones that are found at the gel's surface. This effect is illustrated in Figure 2c, which shows size distributions of particles crossing the gel's boundary calculated for two different activation times.

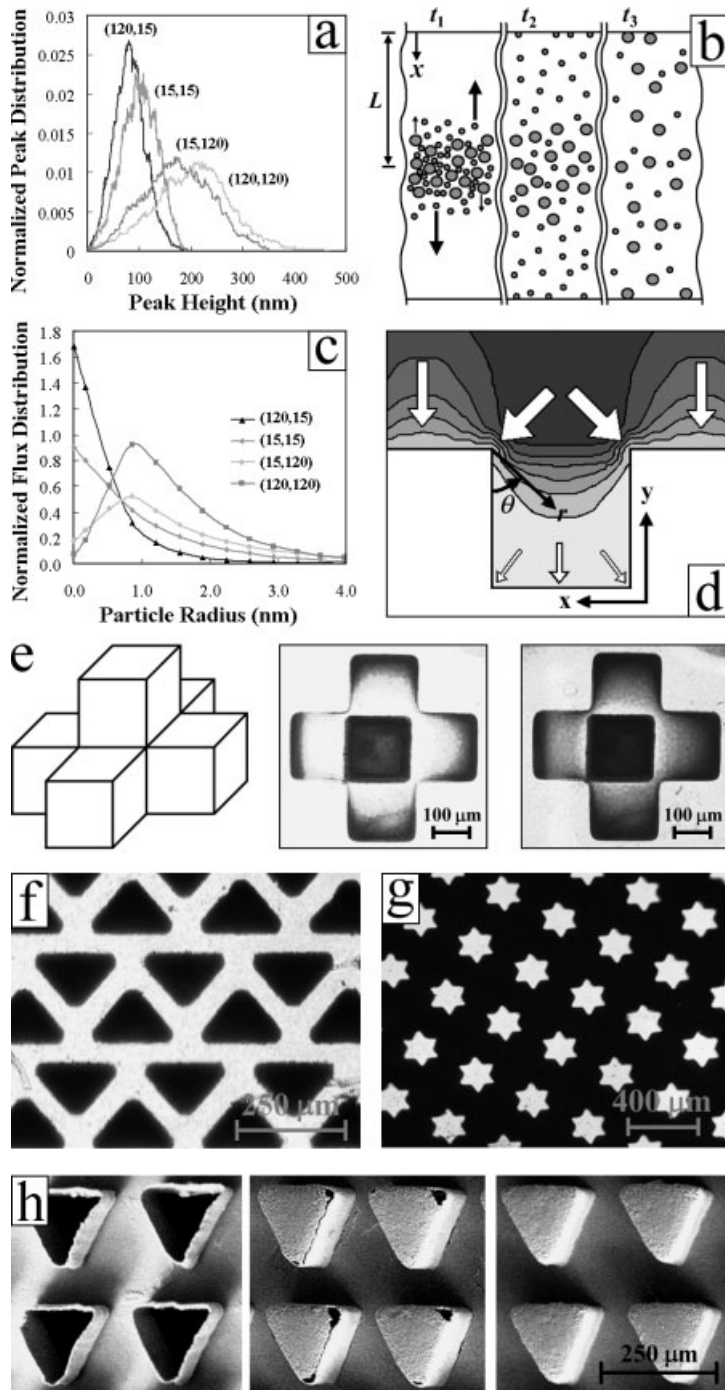


Figure 2. a) Normalized distributions of surface roughness (from AFM measurements) for four Cu foils prepared with different times of gel washing, t_{wash} (first number in parentheses, in minutes) and Pd^{2+} soaking, t_{activ} (second number, in minutes). The roughness was measured over three square areas with dimensions of $10\ \mu\text{m} \times 10\ \mu\text{m}$ each. b) Qualitative illustration of the “filtering” of Pd/Sn particles within the gel. At time t_1 , the particles are generated in the bulk of the gel. At time t_2 , the smaller, rapidly diffusing particles reach the surface, and the larger particles remain in the bulk. Finally, at time t_3 , the small particles diffuse out from the gel, while the larger particles reach the surface. L : one half of the gel slab-thickness; x : distance from the gel surface. c) Calculated surface-flux distributions of colloidal particles of different sizes for values of $(t_{\text{wash}}, t_{\text{activ}})$ corresponding to those in (a). Gels soaked for shorter times had mostly small colloidal particles at their surfaces—consequently, the foils deposited on these films were smoother than those on gels soaked for longer times. d) Calculated steady-state profiles of $[\text{Cu}^{2+}]$ in the plating solution outside the gel; darker regions correspond to higher concentrations. Arrows give qualitative magnitudes of the flux of copper cations reaching the gel’s surface: the thicker the arrow, the faster the deposition. The rectangular (x, y) and cylindrical (r, θ) coordinates are used in the analytical analysis detailed in the Supporting Information. e) In accordance with theoretical predictions, metallization of a cross pyramid (left) started at its top surface and external corners (middle) and proceeded toward the inner corners (right). f, g) Selective metallization of raised features: the triangles are posts and the stars are wells. h) SEM images of freestanding foils with triangular wells at various stages of metallization. Because of diffusional limitations, the corners in the wells metallized last. The features in all three panels are of the same size.

When a master that was soaked for a short time (e.g., $t_{\text{activ}} = 15\ \text{min}$) was placed in a plating solution, metal deposition occurred at small-size catalytic seeds at the surface—consequently, the metal foil was smooth. In stamps soaked for longer times (e.g., $t_{\text{activ}} = 120\ \text{min}$), copper was deposited onto larger catalytic grains, and the surface was rougher.

Film Topography: Diffusional fluxes from the plating solution determined which parts of the micropattern on the gel surface metallized. Consider the simple geometry of a stamp

that has an array of parallel lines embossed on its surface (Fig. 2d). The contours shown in the figure are the steady-state concentration profiles established in the plating solution and calculated for the diffusion-limited copper deposition (see Supporting Information). Because the rate of copper deposition is directly proportional to the flux at the gel surface, we expect the metal to be plated most rapidly in places where the concentration gradients are steepest. Specifically, deposition should be fastest at the tops of the array lines

(starting from the corners), and slowest at their bottoms (ending in the corners). These predictions are in agreement with experiment, and are vividly illustrated in optical micrographs in Figures 2e–h. Metallization of cross “pyramids” (Fig. 2e) began at the uppermost face and proceeded through the middle level before finally reaching the bottom surface (compare Figs. 3a,b). In Figure 2f, selective metallization of the tops of raised posts was used to prepare an array of discontinuous metallic polygons. In Figure 2g, the surface was metallized everywhere except in the star-shaped wells, to give a 2D membrane. Structures intermediate between 2D membranes and 3D continuous foils could be prepared by adjusting the plating times. The leftmost picture in Figure 2h ($t_{\text{plate}} \sim 2$ h) shows a freestanding 3D membrane in which only the top portion of the gel and the sidewalls of the triangular wells are fully metallized. When this structure was allowed to metallize further ($t_{\text{plate}} \sim 8$ h; middle picture), the bottoms of the wells, with the exception of the corners and edges, metallized. For even longer plating times ($t_{\text{plate}} \sim 24$ h, rightmost picture), the entire surface was covered.

Aside from the times of plating, there are three other factors that control the metallization process: i) increasing the aspect ratio of the features limits the diffusion of reactants into the grooves of the pattern, and thus promotes metallization of its top portions; ii) diffusional limitations are minimized by placing the stamp on a rotating support immersed in the plating solution (this arrangement, equivalent to that of a rotating-disk electrode,^[35] increases the flux onto the surface, and facilitates surface metallization); and iii) the external and internal diffusional effects can be combined during the activation process by adjusting the concentration of the activating solution. When $[\text{Pd}^{2+}]$ is low, transport of palladium cations into the gel in the grooves between the features is severely limited. As a result, catalytic seeds do not form in the grooves, but only at the tops of the features, which subsequently become the loci of selective copper deposition (even after days of plating). Figure 3 illustrates how these and other effects can be used to prepare various continuous or membrane-like foils.

In summary, we have demonstrated a flexible experimental technique for microfabrication of 3D copper foils. This method relies on electroless deposition on gel masters where—unlike deposition on solid supports—the process can be controlled by reaction-diffusion phenomena both in the plating solution and in the gel; it is these reaction-diffusion phenomena that enable fabrication of foils of different topographies from identical gel supports. The 3D metallic microstructures we prepared, and others similar to them, could be used as fillings in lightweight materials, materials and microstructures with anisotropic mechanical properties, or as microfiltration membranes. We believe that the method could easily be extended to plating other metals, and we have recently demonstrated its applicability to making nickel films from commercially available plating-bath reagents.^[36] Finally, the idea of preparing catalytic seeds in situ in the gels, and controlling their fluxes at the gel boundaries by adjusting the soaking

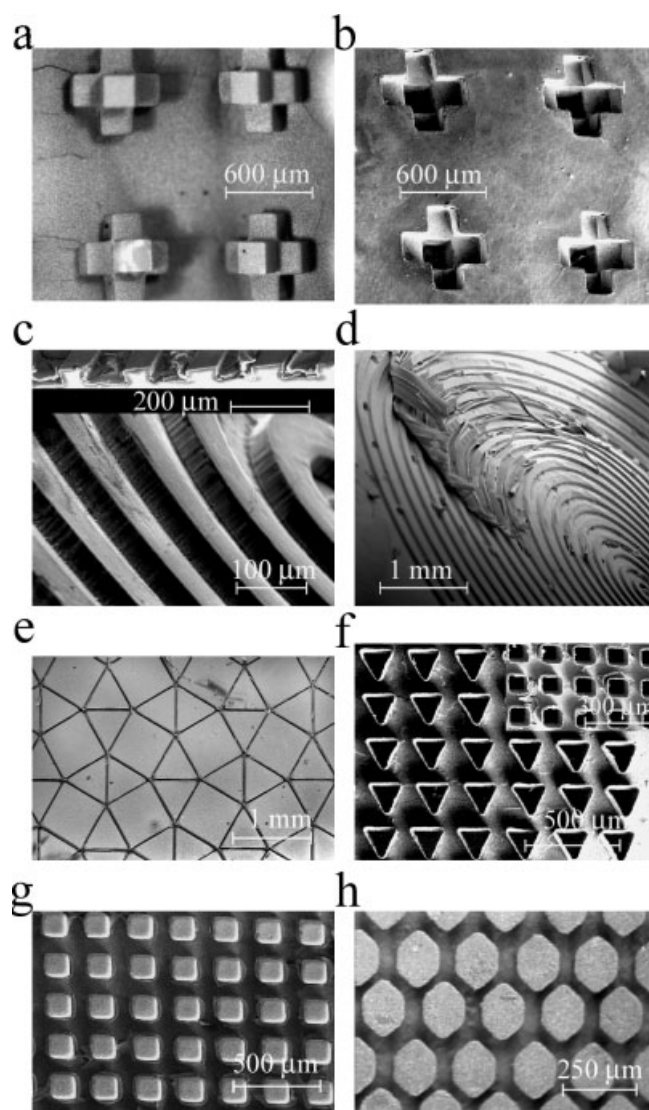


Figure 3. Examples of freestanding 3D copper foils. a) The top surface of a continuous foil with an array of cross pyramids prepared on a 12% agarose master. b) An optical micrograph of the same sheet but viewed from the back side. Note that after cleaning in dilute HCl, the foil was clean and did not have any gel residue even deep in the features. c) Foils prepared on softer agarose stamps (6% in the picture) had smooth top surfaces but often had an even thicker (several μm) layer of gel stuck to their backs, shown peeling in (d). This layer could usually be removed by washing the foils in dilute HCl. The inset in (c) shows the cross-section of the pattern of concentric circles. e) Back side of a cleanly peeled film with sharp, 25 μm grooves. f) 3D membrane-like films with the bottoms of the pattern selectively not metallized. The masters used to prepare these structures were soaked in a low-concentration Pd^{2+} activating solution so that the bottoms of the wells did not metallize even after very long plating times. Fully metallized well features with various aspect ratios ($H/W \sim 0.4$ and 2) are shown in (g) and (h), cleanly peeled from the supporting gel; the bottom and top sides of the films are shown, respectively.

times could be used in printing these seeds onto and activating other supports via the so-called wet stamping method (WETS) we developed.^[37]

Experimental

Modeling and Computational Methods: Details are presented in the Supporting Information.

PDMS Masters: PDMS masters were prepared from Sylgard 184 (Dow) silicone elastomer base and a curing agent mixed in a 10:1 by weight proportion. The mixture was stirred vigorously for 2–3 min, degassed under vacuum, cast against a photolithographically patterned SU8-50 (MicroChem) on silicon, and cured at 60 °C overnight. The PDMS was then gently peeled off and oxidized in a plasma cleaner (Plasma Prep II from SPI, Inc.) for 2 min. The oxidized PDMS was subsequently used as a master for the preparation of agarose replicas.

Typical Metallization Procedure: An agarose plating master was made by casting a hot, 10 w/w solution of agarose against a PDMS master with features $W \sim 50 \mu\text{m}$ wide and $H \sim 50 \mu\text{m}$ deep. The gel was degassed under vacuum for 30–45 s and allowed to gelate at 4 °C for 45 min. The layer of solidified gel was cut into rectangular blocks of dimensions $\sim 2 \text{ cm} \times 2 \text{ cm} \times 2 \text{ mm}$, which were then soaked for $t_{\text{sens}} = 2 \text{ h}$ in aqueous sensitizing solution, washed for $t_{\text{wash}} = 15 \text{ min}$ in deionized water, and soaked in an aqueous activating solution for $t_{\text{activ}} = 30 \text{ min}$. The blocks were then gently dried on tissue paper for 5 s and transferred into a copper plating solution as masters for metal deposition. Their surfaces developed a continuous layer of metal within $t_{\text{plate}} \approx 30 \text{ min}$ from the beginning of plating; at $t_{\text{plate}} \approx 2 \text{ h}$ the metal layer was $\sim 0.7 \mu\text{m}$ thick and could be transferred intact onto a polymeric support (NOA 63). At $t_{\text{plate}} = 24 \text{ h}$, the $\sim 3 \mu\text{m}$ thick foils were rugged enough to be peeled off mechanically from the gel master to yield a freestanding film; the minimal thickness of peelable films was $\sim 2 \mu\text{m}$ after 18 h of plating. Remnants of the gel stuck to the foils were removed by washing with 5 % HCl and ultrasonication for 2–3 min. The gel masters used for plating were not reusable.

Choice of Metallization Materials: Metallization of several other gels (polyacrylamide, poly(acrylic acid) (PAA), gelatin, silica gel, and alginate) was attempted, as well as of PDMS. These gels were not suitable for metallization for various reasons: the alginate dissolved in the developing solution, while others shrank and/or melted, or simply did not metallize. Oxidized PDMS metallized only erratically, mostly on the top portions of the pattern, and the film started to peel off even before nearly-complete metallization was achieved.

Choice of Process Parameters: More concentrated plating solutions than those we used tended to precipitate. Similar effects were observed with elevated temperature or in tall and narrow containers.

Received: June 25, 2004

Final version: October 15, 2004

- [1] M. A. Alodan, L. E. Stover, *Electrochim. Acta* **1999**, *44*, 3721.
- [2] A. L. Coutrot, E. Dufour-Gergam, J. M. Quemper, E. Martincic, J. P. Gilles, J. P. Grandchamp, M. Matlosz, A. Sanchez, L. Darasse, J. C. Ginefri, *Sens. Actuators, A* **2002**, *99*, 49.
- [3] A. L. Coutrot, E. Dufour-Gergam, E. Martincic, J. P. Gilles, J. P. Grandchamp, J. M. Quemper, A. Bosseboeuf, F. Alves, B. Ahamada, *Sens. Actuators, A* **2001**, *91*, 80.
- [4] T. Osaka, N. Takano, T. Yokoshima, *Surf. Coat. Technol.* **2003**, *169*, 1.
- [5] Y. Shacham-Diamand, A. Inberg, Y. Sverdlov, V. Bogush, N. Croitoru, H. Moscovich, A. Freeman, *Electrochim. Acta* **2003**, *48*, 2987.
- [6] M. Strohrmann, P. Bley, O. Fromhein, J. Mohr, *Sens. Actuators, A* **1994**, *42*, 426.
- [7] B. Lochel, A. Maciossek, M. Rothe, W. Windbracke, *Sens. Actuators, A* **1996**, *54*, 663.
- [8] W. K. Schomburg, J. Vollmer, B. Bustgens, J. Fahrenberg, H. Hein, W. Menz, *J. Micromech. Microeng.* **1994**, *4*, 186.
- [9] J. Zaumseil, M. A. Meitl, J. W. P. Hsu, B. R. Acharya, K. W. Baldwin, Y. L. Loo, J. A. Rogers, *Nano Lett.* **2003**, *3*, 1223.
- [10] J. L. Yan, Y. Du, J. F. Liu, W. D. Cao, S. H. Sun, W. H. Zhou, X. R. Yang, E. K. Wang, *Anal. Chem.* **2003**, *75*, 5406.
- [11] I. Rodriguez, P. Spicar-Mihalic, C. L. Kuyper, G. S. Fiorini, D. T. Chiu, *Anal. Chim. Acta* **2003**, *496*, 205.
- [12] D. Dobrev, R. Neumann, N. Angert, J. Vetter, *Appl. Phys. A* **2003**, *76*, 787.
- [13] Y. S. Cheng, K. L. Yeung, *J. Membr. Sci.* **1999**, *158*, 127.
- [14] S. T. Brittain, Y. Sugimura, O. J. A. Schueller, A. G. Evans, G. M. Whitesides, *J. Microelectromech. Syst.* **2001**, *10*, 113.
- [15] I. C. E. Turcu, R. M. Allot, C. M. Mann, C. Reeves, I. N. Ross, N. Lisi, B. J. Maddison, S. W. Moon, P. Prewett, J. T. M. Stevenson, A. W. S. Ross, A. M. Gundlach, B. Koek, P. Mitchell, P. Anastasi, C. McCoard, N. S. Kim, *J. Vac. Sci. Technol. B* **1997**, *15*, 2495.
- [16] S. Koike, F. Shimokawa, T. Matsuura, H. Takahara, *IEEE Trans. Compon., Packag., Manuf. Technol., Part B* **1996**, *19*, 124.
- [17] Y. Saotome, T. Okamoto, *J. Mater. Process. Technol.* **2001**, *113*, 636.
- [18] S. Schiller, K. Goedicke, C. Metzner, *Mater. Sci. Eng. A* **1993**, *163*, 149.
- [19] C. Xirouchaki, R. E. Palmer, *Philos. Trans. R. Soc. London Ser. A* **2004**, *362*, 117.
- [20] P. O'Brien, N. L. Pickett, D. J. Otway, *Chem. Vap. Deposition* **2002**, *8*, 237.
- [21] W. Lee, M. K. Jin, W. C. Yoo, E. S. Jang, J. H. Choy, J. H. Kim, K. Char, J. K. Lee, *Langmuir* **2004**, *20*, 287.
- [22] M. W. Börner, M. Kohl, F. J. Pantenburg, W. Bacher, H. Heln, W. K. Schomburg, *Microsyst. Technol.* **1996**, *2*, 149.
- [23] P. C. Hidber, W. Helbig, E. Kim, G. M. Whitesides, *Langmuir* **1996**, *12*, 1375.
- [24] P. C. Hidber, P. F. Nealey, W. Helbig, G. M. Whitesides, *Langmuir* **1996**, *12*, 5209.
- [25] R. J. Jackman, S. T. Brittain, A. Adams, M. G. Prentiss, G. M. Whitesides, *Science* **1998**, *280*, 2089.
- [26] S. T. Brittain, O. J. A. Schueller, H. K. Wu, S. Whitesides, G. M. Whitesides, *J. Phys. Chem. B* **2001**, *105*, 347.
- [27] R. J. Jackman, S. T. Brittain, G. M. Whitesides, *J. Microelectromech. Syst.* **1998**, *7*, 261.
- [28] W. Goldie, *Plating* **1964**, *75*, 1069.
- [29] Black-Ray UVL-21 compact lamp, UVP Inc, 18.4 W, used at a distance of 1 cm from the sample.
- [30] R. L. Cohen, K. W. West, *J. Electrochem. Soc.* **1973**, *120*, 502.
- [31] J. Israelachvili, *Intermolecular and Surface Forces*, 2nd ed., Academic Press, Boston, MA **2002**.
- [32] R. L. Cohen, K. W. West, *Chem. Phys. Lett.* **1972**, *16*, 128.
- [33] B. Amsden, *Macromolecules* **1998**, *31*, 8382.
- [34] E. M. Johnson, W. M. Deen, *AIChE J.* **1996**, *42*, 1220.
- [35] A. J. Bard, L. R. Faulkner, *Electrochemical Methods: Fundamentals and Applications*, 2nd ed., Wiley, New York **2001**.
- [36] Nickel/Krome plating kit, purchased from Caswell, Inc., www.caswellplating.com.
- [37] C. J. Campbell, M. Fialkowski, R. Klajn, I. T. Bensemann, B. A. Grzybowski, *Adv. Mater.* **2004**, *16*, 1912.
- [38] W. M. Deen, *Analysis of Transport Phenomena*, Oxford University Press, New York **1998**.
- [39] W. H. Press, *Numerical Recipes in C: The Art of Scientific Computing*, 2nd ed., Cambridge University Press, New York **1997**, Ch. 19.